Self-starting passively mode-locked all fiber laser based on carbon nanotubes with radially polarized emission

Yong Zhou,[1] Jian Lin,[1] Xiaoqiang Zhang,[1] Lixin Xu,[1] Chun Gu,[1] Biao Sun,[1] Anting Wang,[1,*] and Qiwen Zhan[2]

[1]*Department of Optics and Optical Engineering, University of Science and Technology of China, Hefei 230026, China*
[2]*Electro-Optics Program, University of Dayton, Dayton, Ohio 45469, USA*
**Corresponding author: atwang@ustc.edu.cn*

Received August 29, 2016; revised October 23, 2016; accepted October 27, 2016;
posted October 27, 2016 (Doc. ID 274777); published November 30, 2016

We demonstrate an all fiber passively mode-locked laser emitting a radially polarized beam by using a few-mode fiber Bragg grating to achieve mode selection and spectrum filtering. An offset splicing of single-mode fiber with four-mode fiber is utilized as a mode coupler in the laser cavity. Carbon nanotubes are introduced into the laser cavity as the saturable absorber to achieve self-start mode locking. The laser operates at 1547.5 nm with a narrow spectrum width of 0.3 nm at 30 dB. The emitted mode-locked pulses have a duration of 22.73 ps and repetition of 10.61 MHz. A radially polarized beam has been obtained with high mode purity by adjusting the polarization in the laser cavity.

OCIS codes: (060.2410) Fibers, erbium; (060.3510) Lasers, fiber; (060.3735) Fiber Bragg gratings; (140.4050) Mode-locked lasers; (160.4236) Nanomaterials.
http://dx.doi.org/10.1364/PRJ.4.000327

1. INTRODUCTION

Radially polarized beams (RPBs) have drawn considerable attention recently due to their interesting properties of symmetrical polarization and amplitude emission [1]. These properties lead to applications in many areas under high numerical aperture (NA) focusing, such as optical trapping [2,3], surface plasmon excitation [4], electron acceleration [5], high resolution metrology [6], and material processing [7,8]. Furthermore, a pulsed RPB is in more demand since most of these applications need high peak power. A variety of spatial polarization selective elements were used in a solid laser cavity to generate continuous-wave (CW) RPBs [9–11]. There have been a few recent papers demonstrating passively mode-locked RPBs in solid lasers with the introduction of mode-locking elements in laser cavities such as graphene absorber [12] or semiconductor saturable absorber (SA) mirror [13].

In fiber lasers, some of our previous works had demonstrated that a few-mode fiber Bragg grating (FM-FBG) is an efficient transverse mode selector when the laser operates within a narrow spectrum [14–16]. For those lasers utilizing FM-FBG as mode selector with hybrid mode injection, high reflection only occurs in a specific narrow wavelength range for different modes [17]. As a result, the fiber laser should operate within a narrow spectrum that matches the spectral properties of the FM-FBG to guarantee high mode purity, while the mostly passively mode-locked fiber laser is operated within a broad spectral range. Several papers have already demonstrated passively mode-locked RPBs based on artificial SAs, but they face challenges with high sensitivity to polarization and environmental changes. For example, [18] demonstrated a passively mode-locked fiber laser based on the nonlinear polarization rotation mechanism. However, the spectrum width under the mode-locked state was so much wider than the FBG reflection range that the mode purity of the pulsed RPB was low. Reference [19] demonstrated a long figure-8 cavity fiber laser generating a rectangular pulse with radially polarized emission based on a nonlinear amplifying-loop mirror; however, the laser structure was relatively complicated. Our group also demonstrated actively mode-locked RPB pulses to evade the sensitivity of polarization [20], but the pulse duration was limited by the modulator, leading to low peak power. Thus true SAs may be more suitable for passively mode-locked RPB fiber lasers. Among variable true SAs, carbon nanotubes (CNTs) offer good stability, wide operating wavelength, and insensitivity of polarization and ease of fabrication [21], and they are chosen as the SA in this work to generate passively mode-locked RPB pulses.

In this paper, we demonstrated a ring cavity all fiber passively mode-locked laser based on CNT that is capable of producing high purity pulsed RPB output. A self-started mode-locked pulse laser with narrow spectral width is successfully demonstrated with a repetition rate of 10.61 MHz and pulse duration of 22.73 ps under stable state. An RPB with high mode purity of 98.03% is obtained through adjusting the polarization in the laser cavity. Compared with the aforesaid mode-locked RPB fiber lasers, this laser integrates all the advantages of self-starting, high peak power, compact structure, high mode purity, and insensitivity to polarization.

2. EXPERIMENTAL SETUP

Figure 1 shows the schematic of the proposed fully integrated fiber laser. A highly erbium-doped fiber (EDF, Liekki Er110-8/125) with a length of 70 cm is pumped by a 974 nm laser diode (LD) though a 974/1550 nm wavelength division multiplexer (WDM). A 9:1 optical coupler (OC) is placed behind the EDF for temporal and spectral property detection. The

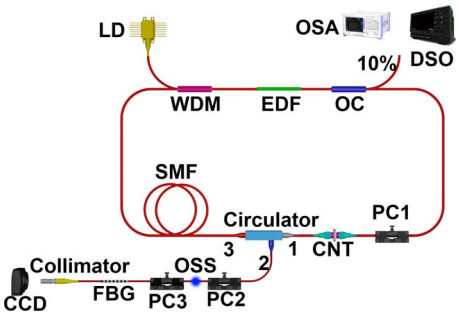

Fig. 1. Schematic of the proposed fiber laser and detection devices.

spectral property of the laser was measured by an optical spectrum analyzer (OSA, ANDO AQ6317B) with a resolution of 0.01 nm from the 10% arm of the coupler. Also from this arm, the temporal properties were measured by a 10 GHz photoelectric probe and a 4 GHz digital storage oscilloscope (DSO, LECTOY Waverunner 640Zi); the autocorrelation trace was measured by an autocorrelator (APE Pulse Check), and the radio frequency (RF) spectrum was measured by an RF analyzer. The single-wall CNT polyvinyl alcohol (PVA) based SA is placed between two fiber connectors behind the output coupler. The CNT-PVA film is fabricated similar to [22], with a modulation depth of ~21.7% and saturation intensity of ~49.7 MW/cm^2. The pulses randomly generated in the laser will be effectively narrowed by the passive saturable absorption. Only the pulses with a repetition rate matched with the cavity length can get stable narrowing and achieve stable mode-locking operation. In addition, the saturable absorption mechanism is insensitive to the laser polarization. A polarization controller (PC1) is connected before the CNT to adjust the injected polarization.

A circulator is used to ensure the unidirectional propagation (clockwise) within the laser cavity with a four mode FBG connected to its port 2. The FBG was fabricated in hydrogen loaded four mode fiber by the phase mask method with a UV excimer laser. The fundamental to fundamental mode reflection wavelength is 1547.5 nm, corresponding to a grating period of 530 nm. The core and cladding diameters of the four-mode fiber are 19 and 125 μm, respectively, with an NA of 0.12; thus the fiber can support four linearly polarized (LP) modes around 1550 nm. The four modes are the LP$_{01}$ mode (defined as the first order mode), the LP$_{11}$ mode (defined as the second order mode), and the LP$_{21}$ and LP$_{02}$ modes (defined as the third order modes), respectively. Figure 2 shows the reflection spectrum of the FBG. There are five reflection peaks within

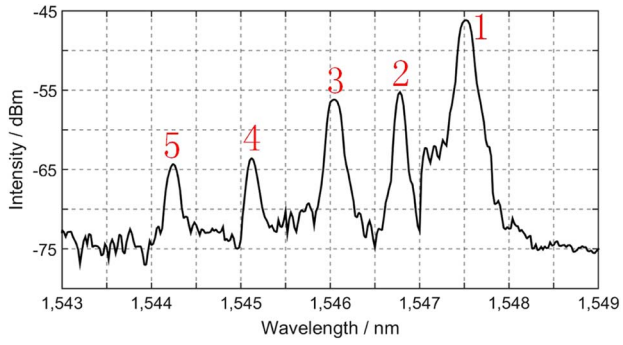

Fig. 2. Reflection spectrum of the four-mode FBG with hybrid mode injection.

the spectrum corresponding to five reflections between different order modes, with peak 1 for the first to first order mode reflection, peak 2 for the 1st to 2nd order mode reflection, peak 3 for the second to second order mode reflection, peak 4 for the second to third order mode reflection, and peak 5 for the third to third order mode reflection. We choose the four mode fiber instead of two mode fiber for FBG fabrication because the cutoff wavelength is far from the laser emission, which ensures the strong guidance of LP$_{11}$ mode. An offset splice spot (OSS) is created between the FBG and the circulator through splicing two sections of fiber (single mode and four modes) with a little lateral misalignment (around 4 μm) to achieve efficient mode coupling from the fundamental mode to the desired high order modes. Two PCs (PC2 and PC3) are placed in front and behind the OSS to adjust the polarization of the injected light and refine the mode distribution of the coupled light. The output mode profiles are record by a CCD camera (Appscintech, CMLN-13S2M-CS) at the FBG end through a fiber collimator. The total length of the cavity was adjusted to be about 19 m by splicing a section of single mode fiber (SMF) between the circulator and the WDM. The whole cavity can be divided into two parts, the longitude mode locking part with SMF (before the OSS) and the transverse mode selection part with few mode fiber (after the OSS).

3. EXPERIMENTAL RESULTS

Through increasing the pump power, the laser can self-start operating at mode locking state; through adjusting the intracavity PC1, the stability of the pulses can be refined to a better state. Furthermore, PC2 and PC3 have a minimal influence on the mode-locking mechanism. Thus, the desired pulsed RPB can be easily obtained. For an input pump power of 302 mW, the emitted pulsed RPB had an average output power of 5.32 mW from the collimator; the laser power from the 10% arm of the OC was measured to be 11.21 mW, which means the intracavity power is 100.89 mW. The autocorrelation trace of the output single pulse is shown in Fig. 3(a), which has a full width-at-half-maximum (FWHM) of about 35 ps. By using sech^2 fitting, the pulse duration was calculated to be 22.73 ps from the autocorrelation trace [23]. Figure 3(b) shows the RF spectrum with a resolution of 12.5 kHz. The fundamental repetition rate is found to be 10.61 MHz, corresponding to a cavity length of 18.9 m. The signal to noise ratio (SNR) is measured to be 75 dB, which ensures good mode-locking stability. The temporal behavior of the steady pulse train is shown in Figs. 4(a) and 4(b) with different time ranges. The interval between adjacent pulses is measured as 94.3 ns, which equals the cavity round trip time.

Figure 5 shows the optical spectrum of the laser at different operation states. The center operating wavelength is 1547.5 nm, corresponding to peak 1 shown in Fig. 2. When the pump power is lower than the self-starting threshold value, which changes with the coupling ratio at the OSS, the laser will operate at CW state with a narrow spectrum width of 0.2 nm at 30 dB and a side-mode suppression ratio (SMSR) of 54 dB. Once the pump power is increased above the self-starting threshold around 170 mW, the laser operates at the mode-locking state. The spectrum width expands to 0.3 nm, and there are other resonances at other reflection peaks of 1546.1 and 1546.8 nm. That leads to the SMSR

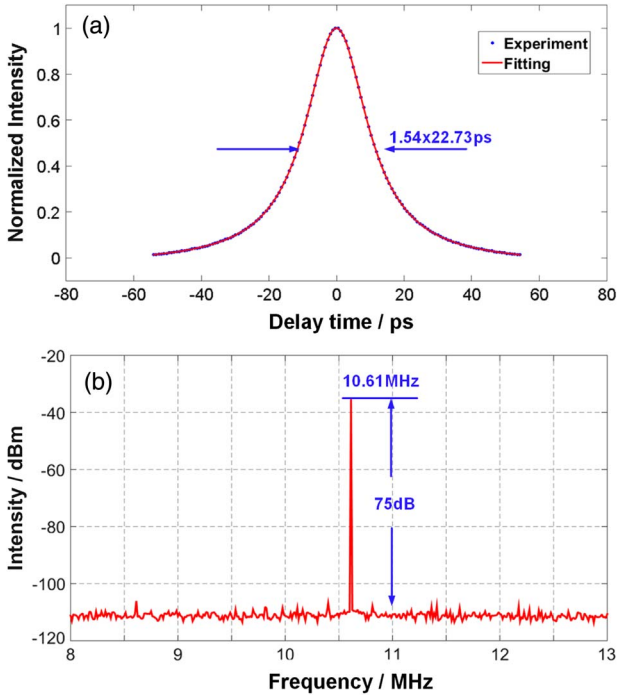

Fig. 3. (a) Autocorrelation trace of single pulse and (b) RF spectrum of the mode locking laser.

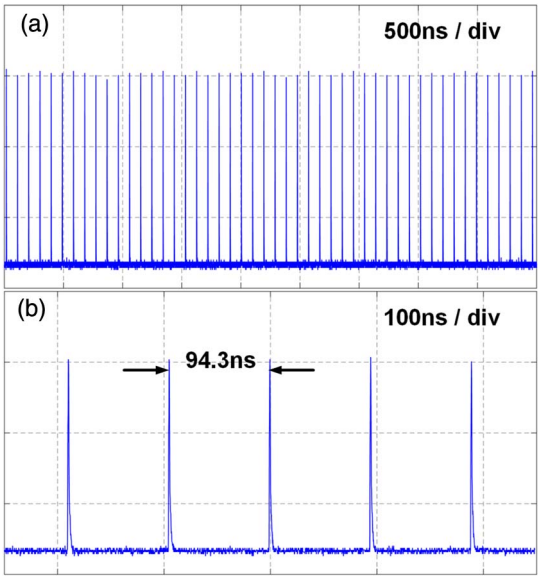

Fig. 4. Pulse train of the passively mode-locked laser in (a) large time range and (b) short time range.

dropping to 45 dB. Even though the optical spectra of both CW and mode-locking states are within the high reflection wavelength range of peak 1 in Fig. 2, the FBG acts as an efficient fundamental mode reflector and only allows the higher modes to pass through, which greatly improves the mode purity of the output beam.

An RPB with high mode purity is obtained through carefully adjusting PC2 and PC3. The mode-locking state can be maintained for weeks during this processing. The intensity profiles of the output laser beam captured by the CCD camera give a

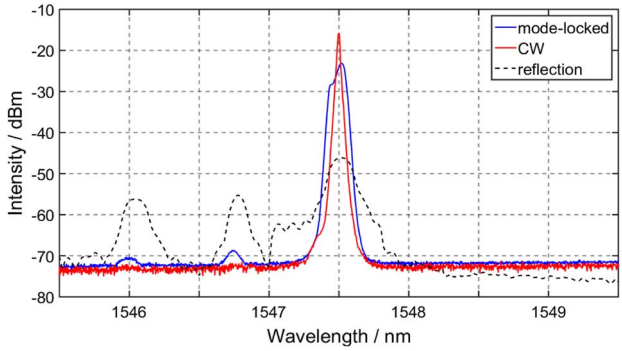

Fig. 5. Optical spectrum of the mode-locked laser (blue solid line), CW operation (red solid line), and the four mode reflection (black dashed line).

doughnut shape as shown in Fig. 6(a). Intensity distributions of the beam after passing through a linear polarizer under four different orientations are shown in Figs. 6(b)–6(e), respectively. Considering the fact that the coupling ratios of the OSS and OC will not change with the optical intensity under a given polarization, the output beam from the collimator have the same pulse properties as the 10% port of the OC. To clarify the pulse property of the RPB, we detect the temporal behavior from the collimator and obtain the same pulse property with the 10% arm of the coupler. For the same input pump power of 302 mW, the emitted pulse RPB has an average output power of 5.32 mW from the collimator, the pulse energy and peak power are calculated to be 0.5 nJ and 19.38 W. In addition, the coupling ratio of the OSS is 17.58% considering of 30% average transmission of the CNT. We note that the peak power can be further increased with a higher power LD; however, this is not the aim of the present paper.

The mode purity was calculated with a function fitting method. From the situation that the mode reflection of the FBG and the mismatch of LP_{01} mode and LP_{11} differed with the longitude mode, the beam intensity distribution could be considered as an incoherent superposition of the strong LP_{11} mode and weak LP_{01} mode. As recognized from the laser spectra, there is no obvious laser resonance within the high order reflection wavelengths, which means there is no considerable LP_{21} and LP_{02} mode in the cavity; thus we fitted the middle line intensity distribution of the output beam as the following function:

$$I_{\text{total}} = m \cdot J_1^2\left(\frac{r}{a}\right) + n \cdot J_0^2\left(\frac{r}{a}\right), \tag{1}$$

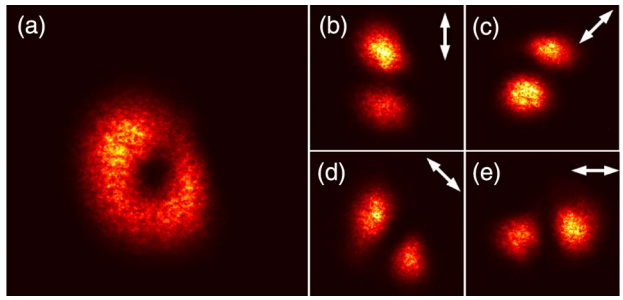

Fig. 6. Intensity distribution of the (a) RPB output; (b)–(e) show the intensity distributions of the output beam after passing through a linear polarizer. Arrow indicates the orientation of the linear polarizer.

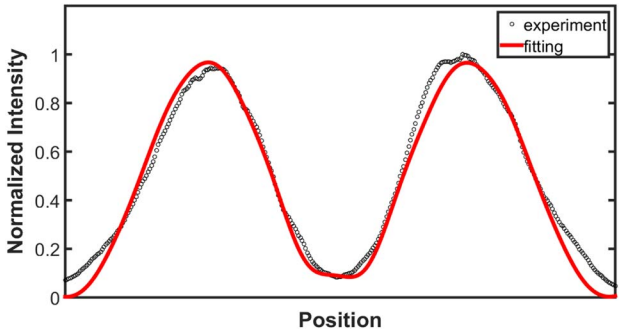

Fig. 7. Function fitting of the output beam intensity distribution. Black circles represents the measured intensity, red line represents the function fitting.

where $J_1(r/a)$ and $J_0(r/a)$ are the first and zeroth order Bessel function, the coefficients m and n represent the ratio of LP_{11} mode and LP_{01} mode, and a is the radius of the fiber core. Figure 7 shows the function fitting of the intensity distribution. The coefficients m and n are found to be 2.839 and 0.09, which indicates a mode purity of the RPB emission of 98.03% through intensity integration.

In summary, we experimentally demonstrated a passively mode-locked all fiber laser that generates RPB emission. The laser is mode locked within a narrow spectrum width (0.3 nm at 30 dB) at the 1547.5 nm operating wavelength, so that the FBG written in the four mode fiber acted as an efficient transverse mode reflector to ensure a high mode purity of 98.03% for the emitted RPB. Self-starting mode-locked operation is realized at a repetition rate of 10.61 MHz, duration of 22.73 ps, and peak power of 19.38 W under a steady state. The emitted pulse RPB could provide a high purity seed to a high power RPB amplifier. It also may find potential applications in mode-division multiplexing system.

Funding. National Natural Science Foundation of China (NSFC) (61275049).

REFERENCES

1. Q. Zhan, "Cylindrical vector beams: from mathematical concepts to applications," Adv. Opt. Photon. **1**, 1–57 (2009).
2. T. Kuga, Y. Torii, N. Shiokawa, T. Hirano, Y. Shimizu, and H. Sasada, "Novel optical trap of atoms with a doughnut beam," Phys. Rev. Lett. **78**, 4713–4716 (1997).
3. M. C. Zhong, L. Gong, D. Li, J. H. Zhou, Z. Q. Wang, and Y. M. Li, "Optical trapping of core-shell magnetic microparticles by cylindrical vector beams," Appl. Phys. Lett. **105**, 181112 (2014).
4. A. Bouhelier, F. Ignatovich, A. Bruyant, C. Huang, G. Colas des Francs, J. C. Weeber, and L. Novotny, "Surface plasmon interference excited by tightly focused laser beams," Opt. Lett. **32**, 2535–2537 (2007).
5. D. N. Gupta, N. Kant, D. E. Kim, and H. Suk, "Electron acceleration to GeV energy by a radially polarized laser," Phys. Lett. A **368**, 402–407 (2007).
6. L. Novotny, M. R. Beversluis, K. S. Youngworth, and T. G. Brown, "Longitudinal field modes probed by single molecules," Phys. Rev. Lett. **86**, 5251–5254 (2001).
7. V. G. Niziev and A. V. Nesterov, "Influence of beam polarization on laser cutting efficiency," J. Phys. D **32**, 1455–1461 (1999).
8. M. Meier, V. Romano, and T. Feurer, "Material processing with pulsed radially and azimuthally polarized laser radiation," Appl. Phys. A **86**, 329–334 (2007).
9. Z. E. Bomzon, G. Biener, V. Kleiner, and E. Hasman, "Radially and azimuthally polarized beams generated by space-variant dielectric subwavelength gratings," Opt. Lett. **27**, 285–287 (2002).
10. R. Zhou, J. W. Haus, P. E. Powers, and Q. Zhan, "Vectorial fiber laser using intracavity axial birefringence," Opt. Express **18**, 10839–10847 (2010).
11. S. Ngcobo, I. Litvin, L. Burger, and A. Forbes, "A digital laser for on-demand laser modes," Nat. Commun. **4**, 2289 (2013).
12. L. Li, Z. Ren, X. Chen, M. Qi, X. Zheng, J. Bai, and Z. Sun, "Passively mode-locked radially polarized Nd-doped yttrium aluminum garnet laser based on graphene-based saturable absorber," Appl. Phys. Express **6**, 082701 (2013).
13. H. Jianhong, D. Jing, C. Yongge, W. Wen, Z. Hui, L. Jinhui, and L. Wenxiong, "Passively mode-locked radially polarized laser based on ceramic Nd:YAG rod," Opt. Express **19**, 2120–2125 (2011).
14. B. Sun, A. Wang, L. Xu, C. Gu, Y. Zhou, Z. Lin, and Q. Zhan, "Transverse mode switchable fiber laser through wavelength tuning," Opt. Lett. **38**, 667–669 (2013).
15. B. Sun, A. Wang, L. Xu, C. Gu, Z. Lin, H. Ming, and Q. Zhan, "Low-threshold single-wavelength all-fiber laser generating cylindrical vector beams using a few-mode fiber Bragg grating," Opt. Lett. **37**, 464–466 (2012).
16. Z. Lin, A. Wang, L. Xu, B. Sun, C. Gu, and H. Ming, "Analysis of generating cylindrical vector beams using a few-mode fiber Bragg grating," J. Lightwave Technol. **30**, 3540–3544 (2012).
17. T. Mizunami, T. V. Djambova, T. Niiho, and S. Gupta, "Bragg gratings in multimode and few-mode optical fibers," J. Lightwave Technol. **18**, 230–235 (2000).
18. J. Dong and K. S. Chiang, "Mode-locked fiber laser with transverse-mode selection based on a two-mode FBG," IEEE Photon. Technol. Lett. **26**, 1766–1769 (2014).
19. B. Sun, A. Wang, C. Gu, G. Chen, L. Xu, D. Chung, and Q. Zhan, "Mode-locked all-fiber laser producing radially polarized rectangular pulses," Opt. Lett. **40**, 1691–1694 (2015).
20. Y. Zhou, A. Wang, C. Gu, B. Sun, L. Xu, F. Li, and Q. Zhan, "Actively mode-locked all fiber laser with cylindrical vector beam output," Opt. Lett. **41**, 548–550 (2016).
21. A. Martinez and Z. Sun, "Nanotube and graphene saturable absorbers for fibre lasers," Nat. Photonics **7**, 842–845 (2013).
22. Y. Sakakibara, A. G. Rozhin, H. Kataura, Y. Achiba, and M. Tokumoto, "Carbon nanotube-poly (vinyl alcohol) nanocomposite film devices: applications for femtosecond fiber laser mode lockers and optical amplifier noise suppressors," Jpn. J. Appl. Phys. **44**, 1621–1625 (2005).
23. C. K. Nielsen, "Mode locked fiber lasers: theoretical and experimental developments," Ph.D. dissertation (Aarhus University, 2006).